



# A Potential Antibody–Drug Conjugate Targeting Human LIV1 for the Treatment of Triple-Negative Breast Cancer

Wei Zhang<sup>1</sup> Hong Liu<sup>1</sup> Wei-Liang Zhuang<sup>1</sup> Yuan Li<sup>1</sup> Li-Ping Xie<sup>1\*</sup> You-Jia Hu<sup>1\*</sup>

<sup>1</sup>Department of Biology, China State Institute of Pharmaceutical Industry Co., Ltd., People's Republic of China

Pharmaceut Fronts 2023;5:e187–e196.

Address for correspondence Li-Ping Xie, PhD, Department of Biology, China State Institute of Pharmaceutical Industry Co., Ltd., Shanghai 20572000, People's Republic of China (e-mail: xieliping@sinopharm.com).

You-Jia Hu, PhD, Department of Biology, China State Institute of Pharmaceutical Industry Co., Ltd., Shanghai 20572000, People's Republic of China (e-mail: bebydou@126.com).

## Abstract

Triple-negative breast cancer (TNBC), which accounts for 15 to 20% of incidents of breast cancer, is the only breast cancer subtype that lacks targeted treatments. It was reported in the literature that LIV1 was highly expressed in TNBC and other solid tumors. This makes LIV1 a potential target for the treatment of TNBC. This study aimed to develop an anti-LIV1 antibody for the treatment of TNBC. In this study, a novel anti-LIV1 antibody Ab1120 was developed and conjugated with monomethyl auristatin E (MMAE) to obtain the antibody–drug conjugate, Ab1120-vcMMAE. The Cell Counting Kit-8 method was used to assess the killing effect of the antibody–drug conjugate on cell lines MDA-MB–231 (high LIV1 expression of breast cancer cell line), MDA-MB-468 (low LIV1 expression of breast cell line), and 293C18 (LIV1-negative human embryonic kidney cell). The antitumor effect of Ab1120-vcMMAE on an MDA-MB-231 xenograft model was determined by evaluating the tumor volume and body weight after its treatment. *In vitro* analysis showed that Ab1120-vcMMAE is a potent inhibitor against the proliferation of a LIV1 overexpression cell line. The *in vivo* results demonstrated its antitumor activity in the cell-derived xenograft breast tumor mouse model. The results of this study suggest that Ab1120-vcMMAE may be used as a new therapeutic drug for patients with LIV1 high-expression breast cancer.

## Keywords

- ▶ triple-negative breast cancer
- ▶ LIV1
- ▶ anti-LIV1 antibody
- ▶ antibody–drug conjugates

## Introduction

Breast cancer is one of the most common malignant tumors and the leading cause of cancer-related mortality in women.<sup>1</sup> According to the data of the World Cancer Research Foundation, more than 2 million cases of breast cancer were diagnosed worldwide in 2020, among which triple-negative breast cancer (TNBC; human epidermal growth factor receptor 2 [Her 2]-negative, estrogen receptor [ER]-negative, and progesterone receptor [PR]-negative) accounting for 15 to

20%. However, the treatments for TNBC are very limited. Currently, chemotherapy, radiation, and surgery are first-line treatments. Thus, there is an urgent need for effective treatments for TNBC.

Antibody–drug conjugate (ADC) is a new drug form that combines the targeting properties of antibodies with the toxicity of small molecules. After nearly 20 years of development, ADC has been a mature technology. Up to 2022, 14 ADCs had received marketing approval.<sup>2</sup> Furthermore, many ADC drugs related to breast cancer have been launched or

received  
March 30, 2023  
accepted  
July 24, 2023  
article published online  
August 24, 2023

DOI <https://doi.org/10.1055/s-0043-1772703>.  
ISSN 2628-5088.

© 2023. The Author(s).

This is an open access article published by Thieme under the terms of the Creative Commons Attribution License, permitting unrestricted use, distribution, and reproduction so long as the original work is properly cited. (<https://creativecommons.org/licenses/by/4.0/>)  
Georg Thieme Verlag KG, Rüdigerstraße 14, 70469 Stuttgart, Germany

entered clinical trials. For example, Seagen has developed an anti-LIV1 ADC, which has shown good efficacy in clinical trials for locally advanced or metastatic TNBC in phase II.<sup>3</sup>

LIV1 (SLC39A6 or ZIP6, solute carrier family 39 member 6), whose coding gene is located on chromosome 18q12.2, is a multiple transmembrane protein. It belongs to the zinc transporter SLC39A family that has a zinc transporter and metalloproteinase activity.<sup>4,5</sup> LIV1 was initially identified as an estrogen-inducible gene in breast cancer cell line ZR-75-1,<sup>6</sup> so it is believed to be closely related to the occurrence and development of breast cancer. There are pieces of evidence that LIV1 interacts with the transcription factors STAT3 and Snail to down-regulate the expression of E-cadherin and to promote epidermal-to-mesenchymal transition.<sup>7,8</sup> In addition, the expression of LIV1 has also been found in other solid tumors such as colon cancer, prostate cancer, and stomach cancer.<sup>9-11</sup> Compared with tumor tissues, the expression level of LIV1 is very low in normal tissues.<sup>12</sup> Therefore, LIV1 can be a potential target for the treatment of cancer.

In this study, we immunized mice with extracellular N-terminus (residues 1–329) of human LIV1, screened and humanized the mouse antibody, and conjugated it via a cleavable dipeptide linker to monomethyl auristatin E (vcMMAE). The resulting ADC was proved to be a potential therapeutic agent for TNBC.

## Materials and Methods

### Materials

Cell lines MDA-MB-231 (Her 2, ER- and PR-negative) and MDA-MB-468 (Her 2, ER- and PR-negative) were purchased from American Type Culture Collection. Cell lines 293C18 (human embryonic kidney cell) and Expi293 are maintained, and the plasmid of pcDNA 3.1, goat anti-human immunoglobulin G (IgG) or goat anti-mouse IgG antibodies, Zenon pHrodo iFL Green Human IgG Labeling Reagent, Fetal bovine blood serum, Dulbecco's Modified Eagle Medium, and Hybridoma SFM were purchased from Thermo Fisher Scientific (Shanghai, China). CD05 medium for Expi293 was purchased from Shanghai OPM Biosciences Co., Ltd (Shanghai, China). Protein G and Protein A were purchased from Global Life Sciences Technologies (Shanghai) Co., Ltd (Shanghai, China). Matrigel (Basement Membrane) was purchased from Corning China. Cell Counting Kit-8 (CCK-8) and vcMMAE were purchased from MedChemExpress (Shanghai, China). Jurkat Recombinant cell was purchased from BPS bioscience, United States. Bright-Glo Luciferase Assay System was purchased from Promega Biotech Co., Ltd (Beijing, China). BALB/c mice and BALB/c nude mice were purchased from Shanghai BK/KY Biotechnology Co., Ltd. (Shanghai, China). Ab1120 is the anti-LIV1 antibody obtained in this study. Plasmids pcDNA3.1-HC and pcDNA3.1-KC were synthesized by GENEWIZ, Inc. (Suzhou, China).

### Generation and Screening of Murine Anti-LIV1 Monoclonal Antibodies

The anti-human LIV1 antibodies were generated by immunizing BALB/C female mice with recombinant extracellular N-terminus (residues 1–329) of human LIV1 (h-LIV1) protein

following the established protocol.<sup>13</sup> The spleen cells of immunized mice were later fused with the myeloma cell line SP2/0. The positive hybridoma cells, secreting LIV1-specific antibodies, were screened by enzyme-linked immunosorbent assay (ELISA) and MDA-MB-231 cell-binding assay. Subsequently, the positive clones were isolated and expanded in the Hybridoma SFM medium. For additional functional assays, monoclonal antibodies (mAbs) were purified from clonal supernatant by protein G affinity chromatography, with the steps including: (1) washing the column with 5 times the volume of phosphate-buffered saline (PBS); (2) sample loading; (3) washing the column with 10 times the volume of PBS; (4) washing the column with 3 times the volume of PBS containing NaCl (1 mol/L); (5) washing the column with 5 times the volume of PBS; (6) elution of the target protein with a citrate buffer (pH = 3.6).

### Humanization and Maturation of Anti-LIV1 mAbs

The sequences of murine antibody variable regions were amplified from candidate hybridomas by reverse transcription-polymerase chain reaction. Next, variable region sequences of murine antibodies were aligned against the human germline database (<https://www.ncbi.nlm.nih.gov/igblast/index.cgi>), and the closest human immunoglobulin germlines were selected as the frameworks. Complementarity-determining regions (CDRs) from the murine mAb were grafted to a human framework template. Then, we designed new VL or VH by back mutation of different potentially important framework residues, which were described previously.<sup>14,15</sup> Subsequently, a series of whole humanized antibodies were obtained by pairing these VL and VH. Finally, affinity maturation antibodies were screened by protein binding and cell binding.

### Generation of Anti-LIV1 Antibody Liv22 as a Positive Control

The sequences of heavy-chain variable region and light-chain variable region of Seagen antibody AbLiv22, which was described previously,<sup>16</sup> was synthesized and constructed onto pcDNA3.1-HC plasmids containing human IgG1 heavy-chain constant region and pcDNA3.1-KC plasmids containing human IgG1 light-chain constant region, respectively. pcDNA3.1-HC-Liv22, and pcDNA3.1-KC-Liv22 plasmids were obtained and transfected to Expi293 cells. AbLiv22 was purified from the supernatant by protein A affinity chromatography, following the same procedure mentioned above.

### Protein Binding Assay

A 96-well plate containing hLIV1 protein (1 µg/mL) was incubated at 4°C overnight. The next day, the plate was blocked with 1% (w/v) bovine serum albumin (BSA)/PBS for 1 hour at 37°C and was washed with PBST (PBS with 0.05% TWEEN 20, v/v) twice. Next, 100 µL antibody dilutions or hybridomas were added to each well, and the plate was incubated for 1 hour at 37°C. The plate was washed again with PBST twice, and 100 µL of goat anti-human IgG or goat anti-mouse IgG antibodies (diluted at a 1:10,000 ratio with 1% (w/v) BSA/PBS) was added for 1 hour at 37°C. The plate was

**Table 1** Chromatographic column and mobile phase

Chromatographic column is MabPac HIC-Butyl (5 $\mu\text{m}$ , 4.6 mm $\times$ 100 mm)					
Mobile phase A (pH = 7.0)	Mobile phase B (pH = 7.0)	Column temperature ( $^{\circ}\text{C}$ )	Flow rate (mL/min)	Injection volume ( $\mu\text{L}$ )	The wavelength of detection (nm)
7.82 mmol/L $\text{NaH}_2\text{PO}_4$ ; 12.2 mmol/L $\text{Na}_2\text{HPO}_4$ ; 1 mol/L $(\text{NH}_4)_2\text{SO}_4$	6.2 mmol/L $\text{NaH}_2\text{PO}_4$ ; 9.78 mmol/L $\text{Na}_2\text{HPO}_4$ ; 20% isopropanol	30	0.5	10	280

washed with PBST four times and then incubated with 100  $\mu\text{L}$  tetramethylbenzidine (TMB) substrate for 5 to 15 minutes. Finally, the optical density (OD) value at 450 nm ( $\text{OD}_{450}$ ) was measured with Microplate Reader. The half-maximal effective concentration ( $\text{EC}_{50}$ ) was calculated using nonlinear regression analysis (GraphPad Prism 5 software).

### Cell Binding Assay

LIV1-expressing MDA-MB-231 cells were added in each well of 96-well u-bottom plates at a density of  $10^5$  cells/well. After a 1,500-rpm centrifugation for 5 minutes, cells were re-suspended in 100  $\mu\text{L}$  1% (w/v) BSA/PBS that contains different concentrations of antibodies, and were incubated for 1 hour on ice. Plates were washed with PBS two times. 100  $\mu\text{L}$  of goat anti-human IgG or goat anti-mouse IgG antibodies (diluted at a 1:10,000 ratio with 1% (w/v) BSA/PBS) was added and plates were incubated for 1 hour on ice. The plates were again washed with PBS four times and then incubated with 100  $\mu\text{L}$  TMB substrate for 5 to 15 minutes. Finally,  $\text{OD}_{450}$  was measured with a Microplate Reader (Biotek, Vermont, United States).

### Conjugation of Antibody

The anti-LIV1 antibody (Ab1120 and AbLiv22) and negative control human antibody (isotype, LIV1 negative) were incubated with tris(2-carboxyethyl)-phosphine (TCEP) at  $37^{\circ}\text{C}$  in the presence of 2 mmol/L ethylenediaminetetraacetic acid for 2 hours. The amount of TCEP is four times the molar equivalent of the antibody. Next, vcMMAE was added to the mixed solution of antibody and TCEP. The amount of vcMMAE is eight times the molar equivalent of the antibody and was incubated for 1 hour on ice. Finally, the mixture was desalted to remove TCEP and unreacted vcMMAE, and the buffer was replaced with 20 mmol/L histidine solution.

The drug-antibody ratio (DAR) was determined by hydrophobic interaction chromatography.<sup>16</sup> The chromatographic column and mobile phase are shown in **Table 1**, and the gradient elution conditions are shown in **Table 2**.

### Endocytosis of ADC

Detection of antibody endocytosis is performed by Zenon pHrodo iFL Green Human IgG Labeling Reagent. The Zenon Labeling reagent contains a fluorophore-labeled Fab fragment, which can bind to the Fc portion of the intact IgG antibody. When the antibody is internalized into the lysosome whose environment is acidic, the labeled Fab fragment can emit a fluorescence that has excitation and emission maxima at 505 nm and 530 nm, respectively, and can be detected by

flow cytometry (Beckman Coulter Inc., California, United States).

A 100  $\mu\text{L}$  MDA-MB-231 cells was added to each well of 96-well plates at a density of  $10^4$  cells/well. The next day, 50  $\mu\text{L}$  of culture medium was aspirated, and 50  $\mu\text{L}$  of the labeling complex that contains ADCs and Zenon Labeling reagent was added to each well of the 96-well plate, and the sample at different times was taken to detect fluorescence intensity by flow cytometry.

### Analysis of Antibody-Dependent Cell-Mediated Cytotoxicity Effect

The target cell MDA-MB-231 was added into 96-well plates at a density of  $1.2 \times 10^4$  with 100  $\mu\text{L}$  per well and incubated overnight at  $37^{\circ}\text{C}$  in an incubator containing 5%  $\text{CO}_2$ . The next day, remove the medium from the 96-well plate, add 60  $\mu\text{L}$  of medium containing the naked antibody or ADC to each well in a threefold gradient dilution with a starting concentration of 2  $\mu\text{g}/\text{mL}$ , and then incubate for 1 hour at  $37^{\circ}\text{C}$ . Then add 40  $\mu\text{L}$  of Recombinant Jurkat cells at a density of  $7.5 \times 10^4$  cells per well and incubate at  $37^{\circ}\text{C}$  for 6 hours. The Bright-Glo assay reagent was added to the 96-well plate at 100  $\mu\text{L}$  per well. After 10 minutes at room temperature, the plate was read by Microplate Readers.  $\text{EC}_{50}$  values were calculated using nonlinear regression analysis (GraphPad Prism 5 software).

### Cytotoxicity Assay

Tumor cells were aliquoted in each well of a 96-well plate at a density of  $1.5 \times 10^4$  cells/well, with different concentrations of antibody or ADCs at  $37^{\circ}\text{C}$ . After 96 hours, 10  $\mu\text{L}/\text{well}$  Cell Counting Kit-8 (CCK-8) was added to each well of the 96-well plate. Plates were incubated for 1 hour at  $37^{\circ}\text{C}$ . Finally, the  $\text{OD}_{450}$  was measured with Microplate Reader. The concentrations of treatment required to inhibit 50% of cell growth or survival ( $\text{IC}_{50}$ ) were calculated using nonlinear regression analysis (GraphPad Prism 5 software).

**Table 2** The gradient elution conditions

Time (min)	Mobile phase A (%)	Mobile phase B (%)
0	90	10
5	90	10
23	0	100
33	0	100
40	90	10

### In Vivo Activity Studies

The tumor volume was calculated using the formula  $(A \times B^2)/2$ , where  $A$  and  $B$  are the largest and second-largest perpendicular tumor dimensions, respectively. The mean tumor volume and weight of mice were monitored.

BALB/c nude mice were selected to establish an MDA-MB-231 tumor model. A total of  $10^7$  cells were suspended in PBS and matrigel (1:1, v/v) and injected subcutaneously into the neck of mice. Once tumors reached a mean tumor volume of  $100 \text{ mm}^3$ , mice were injected intraperitoneally every 4 days for a total of four doses with either ADC (5 mg/kg) or antibody (5 mg/kg). Another group was injected with saline as the blank control. A total of 25 nude mice were divided into five groups.

## Results

### Generation and Identification of Anti-LIV1 Mouse Antibodies

Anti-human LIV1 mouse antibodies were obtained using the hybridoma technology. We received 18 antibodies in total, then screened them using affinity to the human-LIV1 protein (hLIV1; ▶Fig. 1A–C and ▶Table 3). Mouse antibodies with

$EC_{50} < 65 \text{ ng/mL}$  were selected for re-screening by cell binding (▶Fig. 1D, E and ▶Table 4). After two screening cycles, two antibodies (L1214–11E2, L0107–9D11) with high affinity and cell binding activity were chosen.

### Humanization of Anti-LIV1 Antibody

Based on the high affinity and specificity against hLIV1, the L0107–9D11 mAb and L1212–11E2 mAb were selected for further humanization. By searching for the best-fit matches using large germline sequence databases of human immunoglobulins, V3–48 and VKI were selected as the human framework donors for VH/VL of L0107–9D11 and L1214–11E2, respectively. After CDR grafting, the final humanized antibodies were named Ab11E2 and Ab9D11. We examined the affinity of the two antibodies to hLIV1 and compared it with the positive control-AbLiv22 (▶Fig. 2). The data showed that three antibodies have similar affinity to hLIV1; the  $EC_{50}$  values of Ab9D11, Ab11E2, and AbLiv22 are 50.19, 54.22, and 68.06 ng/mL, respectively. According to the expression level of Ab9D11 and Ab11E2 in the Expi293 cell line (86 and 199 mg/L, respectively), Ab11E2 had a higher expression and was selected as a template for affinity maturation. The plasmids of different heavy chains (Hc) and light chains

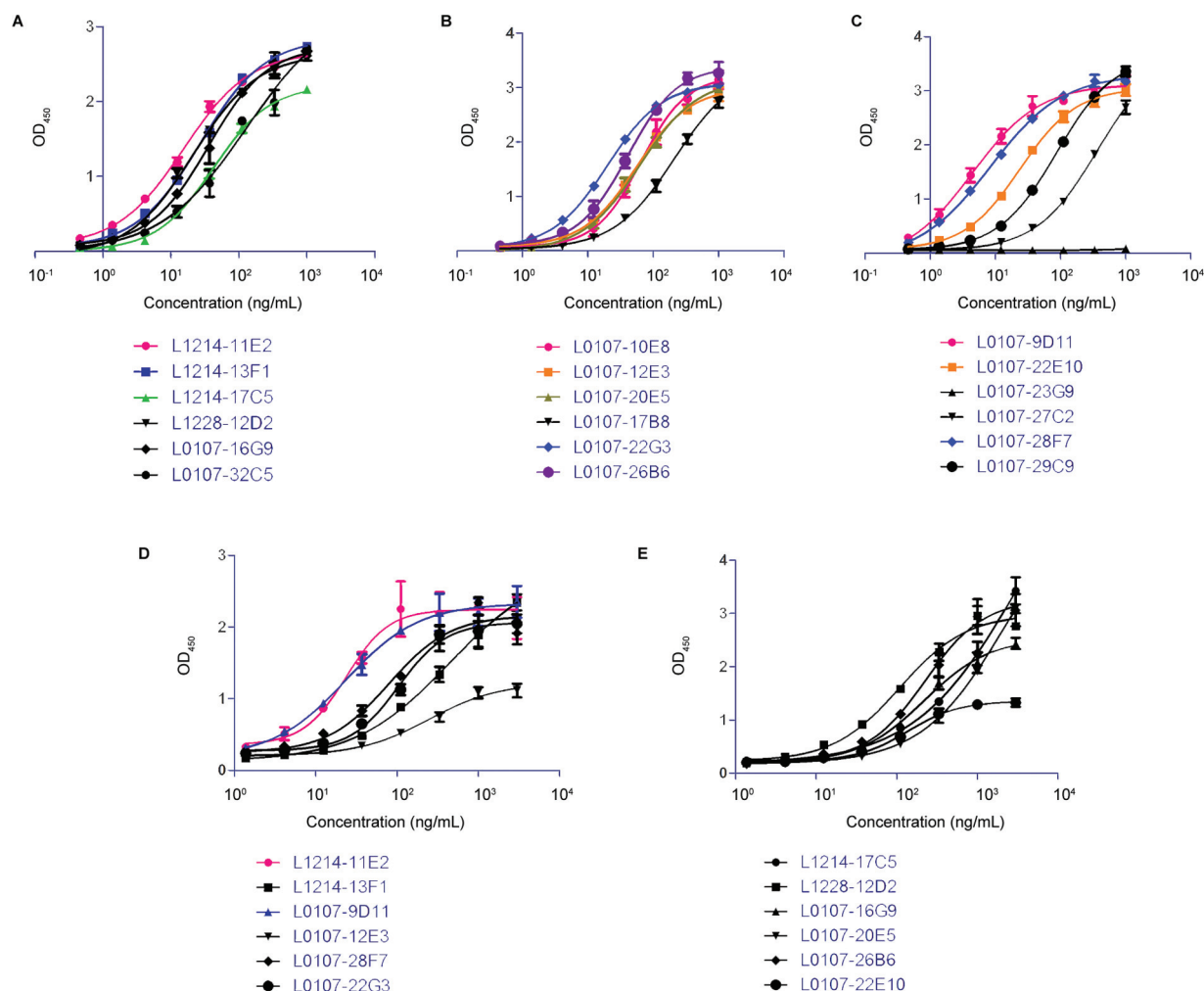


**Fig. 1** Affinity of anti-LIV1 mouse antibodies. (A–C) Protein binding with hLIV1. (D, E) Cell binding. The cell is MDA-MB-231 (a Liv-1-positive cell line).

**Table 3** Affinity of anti-LIV1 mouse antibodies with hLIV1

Antibody	EC <sub>50</sub> (ng/mL)	Antibody	EC <sub>50</sub> (ng/mL)	Antibody	EC <sub>50</sub> (ng/mL)
L1214-11E2	15.23	L0107-10E8	65.23	L0107-9D11	4.42
L1214-13F1	27.23	L0107-12E3	55.08	L0107-22E10	23.94
L1214-17C5	42.12	L0107-20E5	62.24	L0107-23G9	28143
L1228-12D2	21.23	L0107-17B8	212.8	L0107-27C2	369.7
L0107-16G9	35.68	L0107-22G3	19.72	L0107-28F7	8.47
L0107-32C5	127.9	L0107-26B6	40.54	L0107-29C9	88.07

**Table 4** Affinity of anti-hLIV1 mouse antibodies with MDA-MB-231 cell

Antibody	EC <sub>50</sub> (ng/mL)	Antibody	EC <sub>50</sub> (ng/mL)
L1214-11E2	23.57	L0107-10E8	3426
L1214-13F1	457.3	L1228-12D2	108.5
L0107-12E3	247.5	L0107-20E5	2203
L0107-9D11	23.41	L0107-16G9	220.6
L0107-22G3	104.1	L0107-26B6	227.3
L0107-28F7	78.93	L0107-32C5	137.2

(Lc) obtained after site-directed mutagenesis were cross-combined (►Table 5). Different plasmid combinations were transfected into Expi293 cells, and the expressed antibodies were initially screened by protein binding (►Fig. 3A). After humanization, the antigen-binding activity of different antibodies varies greatly, and some antibodies even lose antigen-binding activity (such as Ab1100), which may be caused by the selected back mutation sites. Ab1110, Ab1120, and Ab1122 were selected and other antibodies with higher antigen-binding activity were selected to be further deter-

mined by GatorPlus (Gator Bio) (►Fig. 3B). It was found that the affinity of Ab1120 ( $K_D$ : 3.6E-11M) is much better than the positive control AbLiv22 ( $K_D$ : 1.39E-10M) and chimeric antibody Ab11E2 ( $K_D$ : 1.66E-10M).

#### The Drug–Antibody Ratio, Affinity, and Endocytosis of ADCs

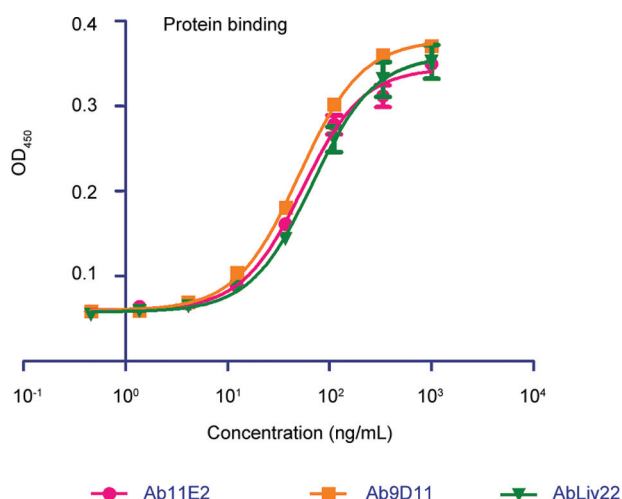
The anti-LIV1 antibody (Ab1120 and AbLiv22) and isotype were conjugated to the vcMMAE with similar DAR values (►Fig. 4A–C and ►Table 6). The data of protein binding showed that the binding affinity to hLIV1 of anti-LIV1 ADCs did not change compared with the naked anti-LIV1 antibody Ab1120 (►Fig. 4D). We took samples at 1, 8, and 24 hours to detect the endocytosis of ADCs by fluorescein isothiocyanate. The data showed that the endocytosis rate of anti-LIV1 ADCs is slow, but a large number of antibodies enter the lysosome at 24 hours (►Fig. 4E).

#### Analysis of ADCC Effect of Ab1120-vcMMAE/Ab1120

We analyzed the ability of antibodies to mediate antibody-dependent cell-mediated cytotoxicity (ADCC) effects by Jurkat Recombinant cells. Compared with Ab1120 (EC<sub>50</sub> of 112.2 ng/mL), the data showed (►Fig. 5) that the ability of the antibody to mediate ADCC effect was not affected after conjugation with vcMMAE (Ab1120-vcMMAE, EC<sub>50</sub> of 133.4 ng/mL).

#### The Killing Effect of ADCs on Cells *In Vitro*

To study the killing effect of ADCs on cells *in vitro*, we selected three cell lines including MDA-MB-231 (high LIV1 expression of breast cancer cell line), MDA-MB-468

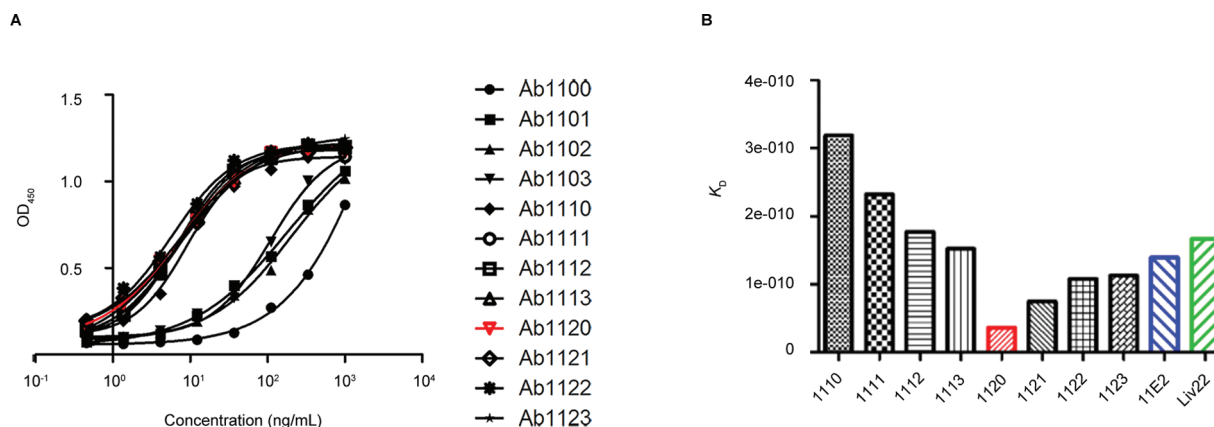


**Fig. 2** Comparison of antibody affinity to h-LIV1. 11E2 and 9D11 are humanized anti-LIV1 antibodies and Liv22 is positive control anti-LIV1 antibody. Data showed that three antibodies had similar affinity to h-LIV1.



**Table 5** Antibodies with different combinations of heavy chain and light chain

Lc Hc	11L0	11L1	11L2	11L3
11H0	1,100	1,101	1,102	1,103
11H1	1,110	1,111	1,112	1,113
11H2	1,120	1,121	1,122	1,123

**Fig. 3** The binding affinity of the humanized anti-LIV1 antibody. (A) ELISA result of the binding affinity between antibody and h-LIV1. (B) Binding analysis of humanized anti-LIV1 antibody by surface plasmon resonance, compared with Ab11E2 and AbLiv22. ELISA, enzyme-linked immunosorbent assay.

(low LIV1 expression of breast cell line), and 293C18 (LIV1-negative human embryonic kidney cell). *In vitro* assays showed that the high LIV1-expressing cell line MDA-MB-231 was strongly sensitive to anti-LIV1 ADCs, the killing effect of Ab1120-vcMMAE (the IC<sub>50</sub> was 37.58 ng/mL) on MDA-MB-231 was better than AbLiv22-vcMMAE (the IC<sub>50</sub> was 42.61 ng/mL), and the 293C18 cell (LIV1 negative) was insensitive to anti-LIV1 ADCs (►Fig. 6C). The killing effect of the low LIV1-expression cell line was observed only at a high concentration (>1,000 ng/mL) (►Fig. 6B). The data showed that the three cell lines are insensitive to naked antibodies (►Fig. 6).

### **In Vivo ADC Activity Study Using MDA-MB-231 Tumors**

In the MDA-MB-231 breast cancer cell xenograft model, after four times of administration with each dose at 5 mg/kg (which is below the average tolerated dose of 10 mg/kg in rodents), we found that both AbLiv22-vcMMAE and Ab1120-vcMMAE could decrease the tumor size (►Fig. 7A) with the tumor suppressive rate being 94.8 and 96.5%, respectively. In addition, the tumor of two mice in the group of Ab1120-vcMMAE became very small. However, only the tumor of one mouse in the group of positive control (AbLiv22-vcMMAE) had the same phenomenon. Tumor growth delay was seen in

**Table 6** The DAR of ADCs

Peak name	Isotype-vcMMAE			hLiv22-vcMMAE			Ab1120-vcMMAE		
	1	2	3	1	2	3	1	2	3
DAR = 0	0.774	2.440	0	0.661	2.965	0	0.636	1.936427	0
DAR = 2	7.834	24.693	49.385	3.553	15.937	31.874	6.116	18.621	37.243
DAR = 4	13.165	41.496	165.984	9.092	40.782	163.129	12.069	36.746	146.986
DAR = 6	6.945	21.891	131.343	5.987	26.855	161.129	8.875	27.022	162.130
DAR = 8	3.008	9.481	75.849	3.001	13.461	107.688	5.148	15.674	125.393
*	4.2			4.6			4.7		

Abbreviations: ADCs, antibody–drug conjugates; DAR, drug–antibody ratio.

Note: \*Average of DAR =  $\sum(\text{weighted peak area})/100$

<sup>1</sup>Area of peak.

<sup>2</sup>Relative area (%).

<sup>3</sup>Weighted peak area = DAR × relative area.

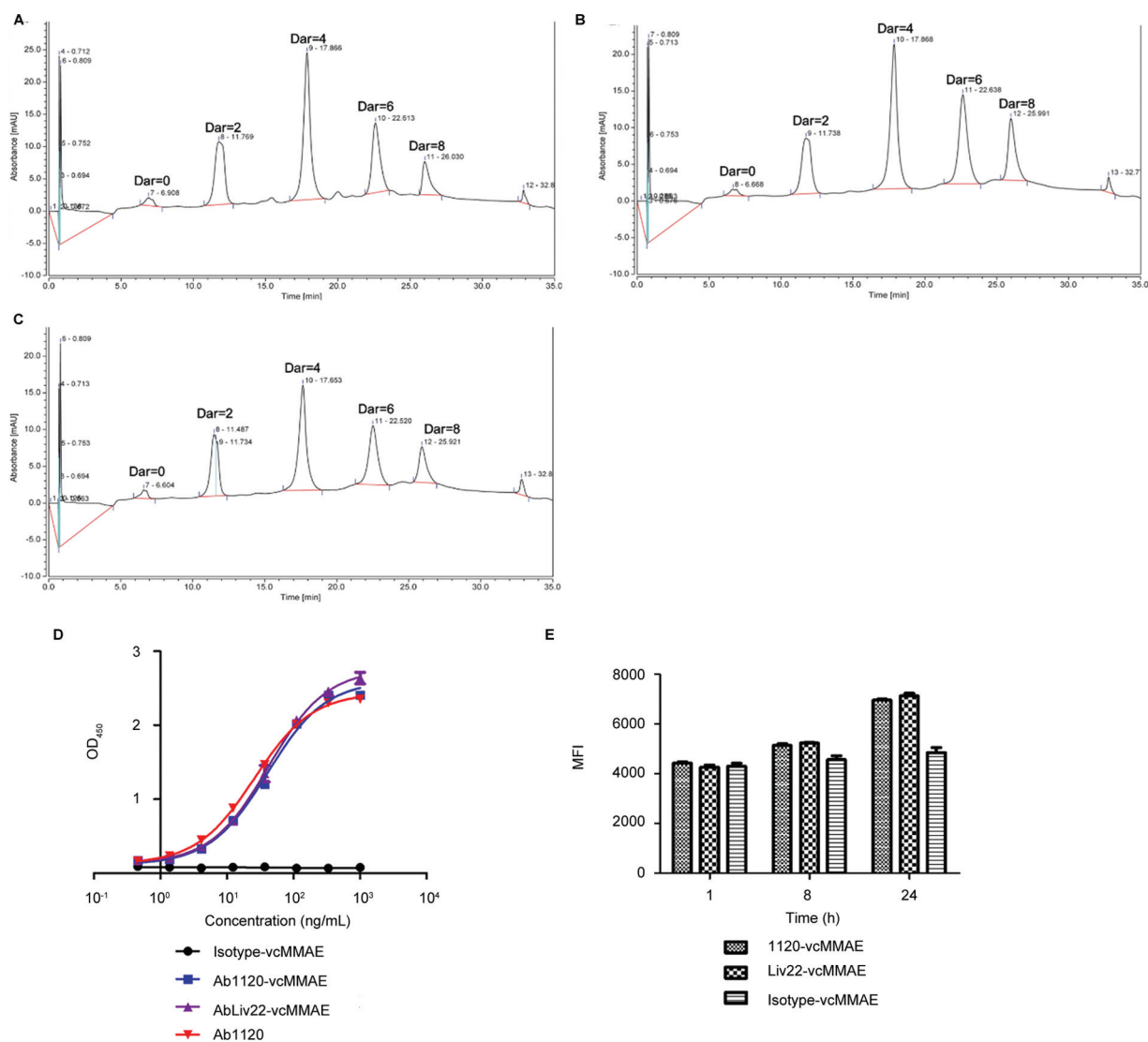


**Fig. 4** DAR of (A) isotype-vcMMAE, (B) Ab1120-vcMMAE, and (C) AbLiv22-vcMMAE. (D) The binding affinity of ADCs to the h-LIV1 was determined by ELISA. (E) Endocytosis of ADCs. ADC, antibody–drug conjugate; DAR, drug–antibody ratio; ELISA, enzyme-linked immunosorbent assay.

the group of negative control, compared with a group of blank. ADC activity without a target has been previously described.<sup>17,18</sup> It involves multiple factors and may be related to the stability of the linker between the antibody and the drug, the microenvironment of the tumor, and the sensitivity of the cell to the released drug.

Compared with the blank group, the body weight of the mice in the four groups did not have statistically significant differences (→ Fig. 7B).

The *in vivo* result suggests that Ab1120-vcMMAE has efficacy and no obvious effect on body weight.

## Discussion

mAbs produced by hybridoma technology have good specificity and high affinity, so hybridoma technology is still one of the main approaches for drug development.<sup>19,20</sup> Since mouse antibodies are prone to HAMA (Human Anti-Murine Antibodies) effects,<sup>20</sup> humanization of mouse antibodies is

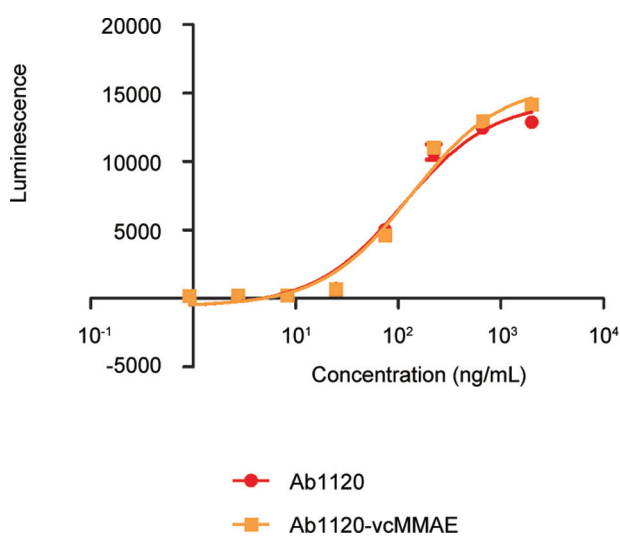


**Fig. 5** Analysis of ADCC effect of Ab1120-vcMMAE/Ab1120. ADCC, antibody-dependent cell-mediated cytotoxicity.

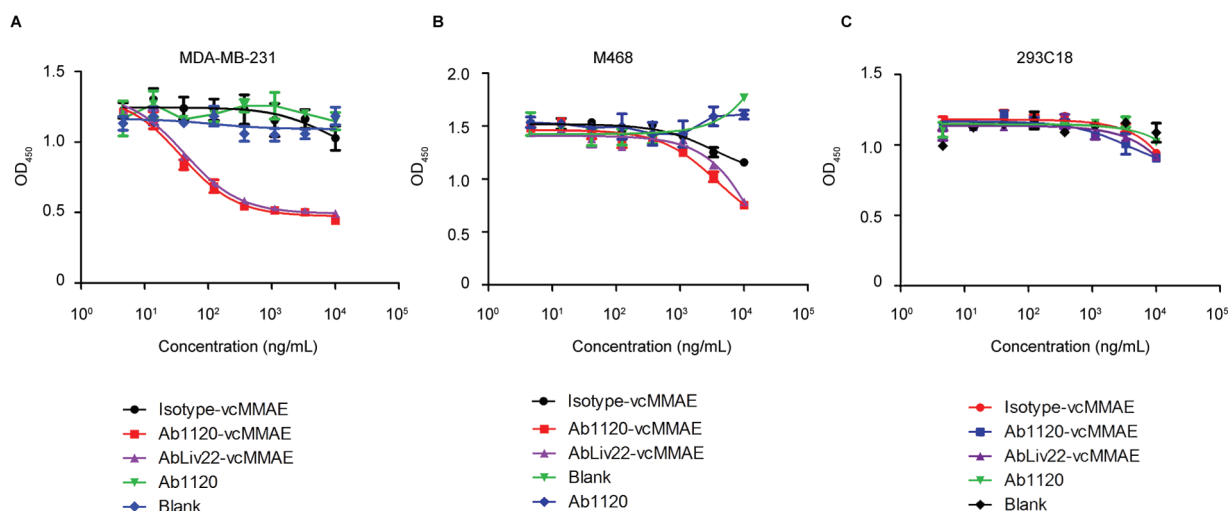


**Fig. 6** CCK-8 demonstrated the effect of ADCs on the proliferation of (A) MDA-MB-231 cells; (B) M468 cells; and (C) 293C18 cells. Ab1120-vcMMAE is Ab1120 conjugated to vcMMAE, Liv22-vcMMAE is AbLiv22 conjugated to vcMMAE, and isotype-vcMMAE is isotype conjugated to vcMMAE. ADC, antibody–drug conjugate.

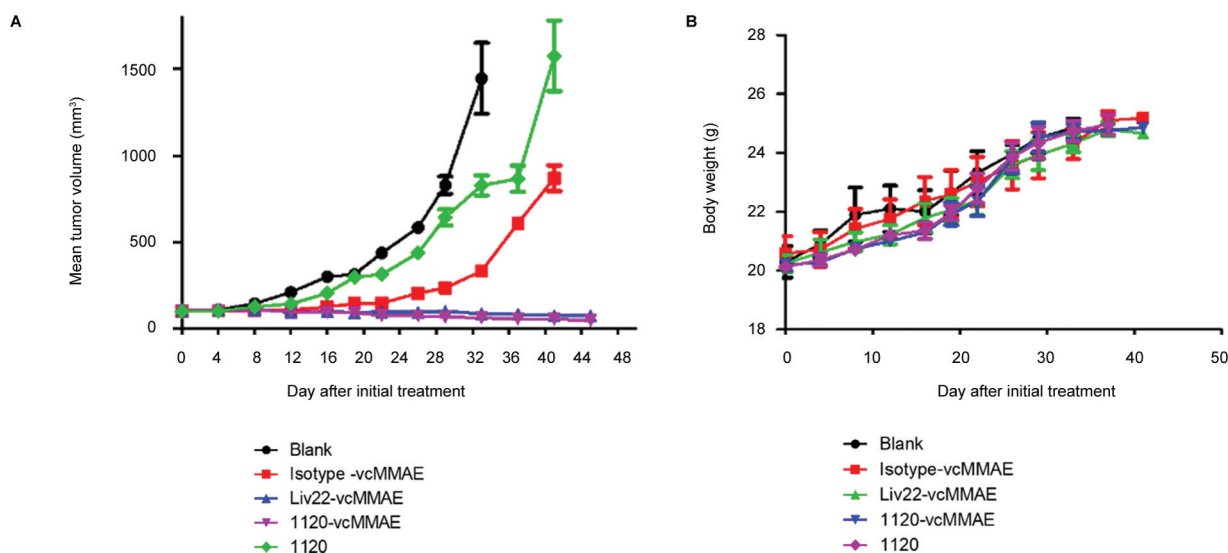


**Fig. 7** (A) Tumor's volume and (B) body weight of the mice after treatment. The drug was administered by injection into the tail vein on days 0, 4, 8, and 12. Note: The blank group (Blank) was injected with normal saline through the tail vein; the negative control group (isotype-vcMMAE) was injected with isotype-vcMMAE through the tail vein; the positive control group (Liv22-vcMMAE) was injected with Liv22-vcMMAE through the tail vein; the 1120-vcMMAE group was injected with 1120-vcMMAE through the tail vein; and the Ab1120 group was injected with Ab1120 through the tail vein.

required. In this study, BALB/C mice were immunized with hLIV1 protein, and the selected mouse antibodies were humanized. Finally, we got an anti-LIV1 antibody Ab1120 whose affinity is better than the positive control AbLiv22, and its humanization rate was above 90%.

ADC is a novel drug form that embellishes antibodies with small-molecule chemotherapeutic drugs through linkers.<sup>21</sup> ADC has the highly targeted nature of antibodies and can also give full play to the cytotoxicity of chemotherapeutic drugs, expanding the window of drug treatment and achieving efficient tumor cell killing.<sup>2</sup> After nearly 20 years of development, and benefiting from progressively mature development technologies, 14 ADCs have been approved, bringing hope for the treatment of patients with different diseases.<sup>22</sup>

However, we also found that ADC drugs currently in clinical development or early development are still focused on a small range of targets, such as Her 2, TROP 2, etc.<sup>23</sup> Taking breast cancer as an example, the current ADC drug development is still focused on Her 2 targets, and it can be said that target homogenization is rather serious. Therefore, the validation and application of new targets is a new way out for innovative ADC development and innovative therapy development. In this article, we focus on the target LIV1, which is the first zinc ion transporter protein found in breast cancer cells that can be induced by estrogen to be expressed, so it is thought to be closely associated with breast cancer development and progression.<sup>3,24–26</sup> Moreover, LIV1 is highly expressed in a variety of tumor cells including breast,



prostate, pancreatic, cervical, and liver cancers with limited expression in normal tissues,<sup>9</sup> and this differential expression level makes LIV1 an ideal target for the development of ADCs.

In this study, we developed an anti-human LIV1 antibody (Ab1120) and conjugated it with vcMMAE to obtain a novel ADC (Ab1120-vcMMAE), which has inhibitory activity against the proliferation of LIV1-expressing cell line and tumor. *In vitro*, Ab1120-vcMMAE has a strong inhibitory effect on the high LIV1-expression cell proliferation. A similar effect on low LIV1-expressing cell lines requires a high concentration (>1,000 ng/mL). The difference in the sensitivity of the low- or high-LIV1 expression cell lines to anti-LIV1 ADCs indicates that the effect of anti-LIV1 ADCs on cells depends on the LIV1 expression level, and also may be related to antigen heterogeneity.<sup>27,28</sup> The *in vivo* data show that Ab1120-vcMMAE is effective in xenograft models of breast cancer with high expression-LIV1 at a dose of 5 mg/kg. Compared with the blank group, the data *in vivo* showed that naked antibody alone (5 mg/kg) had a weaker inhibitory effect on tumor growth, which may be related to ADCC and complement-dependent cytotoxicity. Our other experiments showed that the Ab1120 and Ab1120-vcMMAE have ADCC effect *in vitro* (►Fig. 5). We think this is a promising sign since antibody conjugate to small-molecule toxin does not destroy the ADCC of antibody, which is more helpful for ADC to kill tumor cells and inhibit tumor growth. Although tumor growth delay was seen in the group of negative control (compared with a blank group), this noncancer antigen-dependent activity was observed in many ADC drugs, and it is a continuing topic of study and has been attributed to a combination of factors, including but not limited to the enhanced permeability and retention effect of a tumor, linker's stability of antibody and drug, the microenvironment of the tumor, and the sensitivity of the cell to the released drug. In summary, this study showed that Ab1120-vcMMAE has the potential treatment for TNBC and other LIV1-positive cancer. This study indicated that LIV1 is a promising candidate for ADC therapy because of its high expression level in solid tumors and limited normal tissue expression.

#### Ethical Approval

All animal experiments were approved by the Animal Ethical Committee at the China State Institute of Pharmaceutical Industry, which conformed to the National Institutes of Health Guidelines on Laboratory Research and Guide for the Care and Use of Laboratory Animals (Eighth Edition, 2011). This article does not contain any studies with human participants performed by any of the authors.

#### Conflict of Interest

None declared.

#### References

- Bray F, Ferlay J, Soerjomataram I, Siegel RL, Torre LA, Jemal A. Global cancer statistics 2018: GLOBOCAN estimates of incidence and mortality worldwide for 36 cancers in 185 countries. *CA Cancer J Clin* 2018;68(06):394–424
- Fu Z, Li S, Han S, Shi C, Zhang Y. Antibody drug conjugate: the “biological missile” for targeted cancer therapy. *Signal Transduct Target Ther* 2022;7(01):93
- Saravanan R, Balasubramanian V, Swaroop Balamurugan SS, et al. Zinc transporter LIV1: a promising cell surface target for triple negative breast cancer. *J Cell Physiol* 2022;237(11):4132–4156
- Lopez V, Kelleher SL. Zip6-attenuation promotes epithelial-to-mesenchymal transition in ductal breast tumor (T47D) cells. *Exp Cell Res* 2010;316(03):366–375
- Taylor KM, Morgan HE, Johnson A, Hadley LJ, Nicholson RI. Structure-function analysis of LIV-1, the breast cancer-associated protein that belongs to a new subfamily of zinc transporters. *Biochem J* 2003;375(Pt 1):51–59
- Manning DL, Daly RJ, Lord PG, Kelly KF, Green CD. Effects of oestrogen on the expression of a 4.4 kb mRNA in the ZR-75-1 human breast cancer cell line. *Mol Cell Endocrinol* 1988;59(03):205–212
- Huber MA, Kraut N, Beug H. Molecular requirements for epithelial-mesenchymal transition during tumor progression. *Curr Opin Cell Biol* 2005;17(05):548–558
- Taylor KM, Hiscox S, Nicholson RI. Zinc transporter LIV-1: a link between cellular development and cancer progression. *Trends Endocrinol Metab* 2004;15(10):461–463
- Sussman D, Smith LM, Anderson ME, et al. SGN-LIV1A: a novel antibody-drug conjugate targeting LIV-1 for the treatment of metastatic breast cancer. *Mol Cancer Ther* 2014;13(12):2991–3000
- Unno J, Satoh K, Hirota M, et al. LIV-1 enhances the aggressive phenotype through the induction of epithelial to mesenchymal transition in human pancreatic carcinoma cells. *Int J Oncol* 2009;35(04):813–821
- Tozlu S, Girault I, Vacher S, et al. Identification of novel genes that co-cluster with estrogen receptor alpha in breast tumor biopsy specimens, using a large-scale real-time reverse transcription-PCR approach. *Endocr Relat Cancer* 2006;13(04):1109–1120
- Greenfield EA. Standard Immunization of Mice, Rats, and Hamsters. *Cold Spring Harb Protoc* 2020;2020(03):100297
- Smith ML, Sussman D, Arthur W, Nesterova A. Humanized Antibodies To LIV-1 And Use Of Same To Treat Cancer. U.S. Patent 20130259860A1. June, 2011
- Jones PT, Dear PH, Foote J, Neuberger MS, Winter G. Replacing the complementarity-determining regions in a human antibody with those from a mouse. *Nature* 1986;321(6069):522–525
- Smith ML, Sussman D, Arthur W, Nesterova A. Humanized antibodies to LIV-1 and use of same to treat cancer. US Patent 9228026. January, 2016
- Lyon RP, Meyer DL, Setter JR, Senter PD. Conjugation of anticancer drugs through endogenous monoclonal antibody cysteine residues. *Methods Enzymol* 2012;502:123–138
- Kovtun YV, Audette CA, Ye Y, et al. Antibody-drug conjugates designed to eradicate tumors with homogeneous and heterogeneous expression of the target antigen. *Cancer Res* 2006;66(06):3214–3221
- Boghaert ER, Khandke K, Sridharan L, et al. Tumoricidal effect of calicheamicin immuno-conjugates using a passive targeting strategy. *Int J Oncol* 2006;28(03):675–684
- Parray HA, Shukla S, Samal S, et al. Hybridoma technology a versatile method for isolation of monoclonal antibodies, its applicability across species, limitations, advancement and future perspectives. *Int Immunopharmacol* 2020;85:106639
- Klee GG. Human anti-mouse antibodies. *Arch Pathol Lab Med* 2000;124(06):921–923
- Francisco JA, Cerveny CG, Meyer DL, et al. cAC10-vcMMAE, an anti-CD30-monomethyl auristatin E conjugate with potent and selective antitumor activity. *Blood* 2003;102(04):1458–1465
- Hafeez U, Parakh S, Gan HK, Scott AM. Antibody-drug conjugates for cancer therapy. *Molecules* 2020;25(20):4764
- Li JY, Perry SR, Muniz-Medina V, et al. A biparatopic HER2-targeting antibody-drug conjugate induces tumor regression in

- primary models refractory to or ineligible for HER2-targeted therapy. *Cancer Cell* 2016;29(01):117–129
- 24 Krop IE, Kim SB, Martin AG, et al. Trastuzumab emtansine versus treatment of physician's choice in patients with previously treated HER2-positive metastatic breast cancer (TH3RESA): final overall survival results from a randomised open-label phase 3 trial. *Lancet Oncol* 2017;18(06):743–754
- 25 Grattan BJ, Freake HC. Zinc and cancer: implications for LIV-1 in breast cancer. *Nutrients* 2012;4(07):648–675
- 26 Lue HW, Yang X, Wang R, et al. LIV-1 promotes prostate cancer epithelial-to-mesenchymal transition and metastasis through HB-EGF shedding and EGFR-mediated ERK signaling. *PLoS One* 2011;6(11):e27720
- 27 Romero I, Garrido C, Algarra I, et al. MHC intratumoral heterogeneity may predict cancer progression and response to immunotherapy. *Front Immunol* 2018;9:102
- 28 Vitale I, Shema E, Loi S, Galluzzi L. Intratumoral heterogeneity in cancer progression and response to immunotherapy. *Nat Med* 2021;27(02):212–224